Photochemical Targeting of Epidermal Growth Factor Receptor: A Mechanistic Study

Mark D. Savellano[1,2] and Tayyaba Hasan[3]

[1]Department of Surgery, Dartmouth-Hitchcock Medical Center, Lebanon, New Hampshire; [2]Thayer School of Engineering, Dartmouth College, Hanover, New Hampshire; and [3]Department of Dermatology, Wellman Center for Photomedicine, Harvard Medical School, Massachusetts General Hospital, Boston, Massachusetts

ABSTRACT

Purpose: **Photoimmunotherapy may allow target-specific photodynamic destruction of malignancies and may also potentiate anticancer antibody therapies. However, clinical use of either of the two modalities is limited for different reasons. Antibody therapies suffer from being primarily cytostatic and the need for prolonged administration with consequent side effects. In the case of photoimmunotherapy, a major impediment has been the absence of well-characterized photosensitizer immunoconjugates (PIC). In this investigation, we suggest a strategy to overcome these limitations and present the successful targeting of epidermal growth factor receptor (EGFR) using a well-characterized PIC.**

Experimental Design: **The PIC consisted of the EGFR-recognizing chimeric monoclonal antibody, C225, conjugated with a two-branched polyethylene glycol and benzoporphyrin derivative (BPD, Verteporfin). Mechanistic studies included photophysics, phototoxicity, cellular uptake, and catabolism experiments to yield dosimetric parameters. Target cells included two EGFR-overexpressing human cancer cell lines, OVCAR-5 and A-431. Nontarget cells included an EGFR-negative fibroblast cell line, 3T3-NR6, and a monocyte-macrophage cell line, J774.**

Results: **BPD-C225 PICs targeted and photodynamically killed EGFR-overexpressing cells, whereas free BPD exhibited no specificity. On a per mole basis, PICs were less phototoxic than free BPD, but PICs were very selective for target cells, whereas free BPD was not. Phototoxicity of the PICs increased at prolonged incubations. Photodynamic dose calculations indicated that PIC photophysics, photochemistry, catabolism, and subcellular localization were important determinants of PIC phototoxic potency.**

Conclusions: **This study shows the efficacy of EGFR targeting with PIC constructs and suggests approaches to improve PIC designs and targeting strategies for *in vivo* photoimmunotherapy. The approach offers the possibility of dual effects via antibody-mediated cytostasis and photoimmunotherapy-based cytotoxicity.**

INTRODUCTION

Over the past two decades, there has been a concerted effort to expand the utility of photodynamic therapy (PDT; ref. 1). One approach is to conjugate the photosensitizer to targeting molecules, especially monoclonal antibodies (MAb). Use of photosensitizer immunoconjugates (PIC) in PDT, termed photoimmunotherapy following the pioneering work of Mew et al. in the early 1980s (2), could be particularly useful for treating complex disease sites where prevention of collateral damage is critical. Photoimmunotherapy might also potentiate anticancer antibodies. Because many anticancer antibodies are subcurative as single-agents, they have often been used in combination with chemotherapy or radiation (3–5). Therefore, it is a logical extension to investigate photoimmunotherapy not only as a way to improve the targeting capability of PDT, but also as a means to potentiate anticancer antibody therapies.

To date, photoimmunotherapy has only been studied occasionally *in vivo* (6). Limited preliminary clinical photoimmunotherapy studies were promising but were not conducted systematically (7). Reviews suggest that progress in photoimmunotherapy research has been restricted because functional, well-characterized PICs have been difficult to make (8–11). Many photosensitizers used in PDT are hydrophobic and lipophilic and tend to aggregate in aqueous solutions (12); therefore, conjugating them to antibodies has been cumbersome. Consequently, many of the results obtained in previous photoimmunotherapy studies are difficult to interpret due to the poor quality of the PICs.

In more recent photoimmunotherapy studies, investigators attempted to avert PIC aggregation and increase coupling efficiency by converting the photosensitizer to a water-soluble derivative (13, 14). Similarly, in studies by Levy et al., the first group to make PICs with the potent second-generation photosensitizer, benzoporphyrin derivative (BPD, Verteporfin; refs. 15, 16), it was decided that the photosensitizer must first be attached to a water-soluble polymer prior to conjugation with antibodies (17–21). Despite the promise of these investigations, the conjugations were complicated, and the PICs were still aggregated and most likely contained substantial amounts of noncovalently associated free photosensitizer impurities. Therefore, mechanistic interpretation and utilitization of previous data, including our own, for design of therapeutic regimens is difficult. We have recently devised a simple new method for producing functional, high-purity PICs without having to convert the photosensitizer to a water-soluble derivative (11, 22, 23). The method has been successfully used

Received 9/15/04; revised 11/2/04; accepted 11/23/04.

Grant support: NIH grant R01AR40352, Department of Defense Medical Free Electron Laser Program grant F49620-01-1-0014 (T. Hasan), and by the Whitaker Foundation Biomedical Engineering Graduate Fellowship program (M. Savellano).

The costs of publication of this article were defrayed in part by the payment of page charges. This article must therefore be hereby marked *advertisement* in accordance with 18 U.S.C. Section 1734 solely to indicate this fact.

Requests for reprints: Tayyaba Hasan, Department of Dermatology, Wellman Center for Photomedicine, Harvard Medical School, Massachusetts General Hospital, 40 Blossom Street, BAR 314, Boston, MA 02114. Phone: 617-726-6856; Fax: 617-726-8566; E-mail: thasan@partners.org.

to make anti–epidermal growth factor receptor (EGFR) PICs consisting of the chimeric MAb, C225 (24, 25), conjugated with a 10 kDa two-branched polyethylene glycol and BPD. The BPD-C225 PICs specifically targeted and photodynamically killed EGFR-overexpressing target cells (11, 22, 23), and they retained the receptor-blocking function of native C225.[4] Thus, the BPD-C225 PICs can exert a dual therapeutic effect by selectively targeting photodynamic destruction of EGFR-overexpressing cells and concomitantly blocking EGFR signaling. Because roughly a third of all epithelial tumors overexpress the EGFR (26, 27), the BPD-C225 PICs may be useful for treating a variety of tumor types. Another advantage of the BPD-C225 PICs is that BPD is approved for human use (28), and C225, alone or with radiation or chemotherapy, is approved for metastatic colorectal cancer and is in phase I-III trials for various other cancers (3–5).

To establish photoimmunotherapy as a viable therapeutic regimen, it is critical to establish the utility of PICs as selective PDT agents and to obtain estimates of dosimetric parameters. As a first step toward this end, we conducted detailed photophysics and photobiology-based *in vitro* dosimetry experiments with the BPD-C225 PICs, and for comparison, with free BPD, to assess their efficacy and to examine the underlying mechanisms of EGFR-targeted photoimmunotherapy. We find that photoimmunotherapy efficacy is affected in complex ways by various photochemical and photobiological processes and suggest refinements that could make photoimmunotherapy a valuable therapeutic option.

MATERIALS AND METHODS

Cell Lines. A-431 human epidermoid carcinoma cells and J774 mouse monocyte-macrophage cells were purchased from American Type Culture Collection (Rockville, MD). EGFR-negative variant 3T3-NR6 (NR6) cells (29) were a generous gift from Dr. A. Wells (Department of Pathology, University of Alabama, Birmingham, AL). Maintenance conditions for these cells have previously been described (23). NIH:OVCAR-5 (OVCAR-5) human ovarian cancer cells were purchased from Fox Chase Cancer Institute (Philadelphia, PA) and were maintained under conditions similar to those used for J774 cells.

Antibodies. C225 anti-EGFR chimeric MAb was a generous gift from ImClone Systems Incorporated (Somerville, NJ). Herceptin anti-HER2/ErbB2 humanized MAb was a generous gift from Genentech (San Francisco, CA).

Preparation of Benzoporphyrin Derivative-C225 Photosensitizer Immunoconjugates. PICs were prepared using an optimized procedure previously described elsewhere (11, 22, 23). Briefly, BPD, a generous gift from QLT PhotoTherapeutics Incorporated (Vancouver, BC, Canada), was converted to an *N*-hydroxysuccinimide ester. Prior to BPD labeling, C225 MAb was polyethylene glycolated with a 10 kDa two-branched polyethylene glycol-*N*-hydroxysuccinimide ester (Shearwater Polymers, Huntsville, AL). The BPD-*N*-hydroxysuccinimide ester was then reacted with the polyethylene glycolated C225 MAb.

[4]A.C.E. Moor, et al. Photoimmunotargeting of the epidermal growth factor receptor *in vitro*, Int J Cancer, submitted for publication, 2005.

Determining Benzoporphyrin Derivative-Antibody Molar Ratios of the Photosensitizer Immunoconjugates. BPD-antibody molar ratios of the PICs were determined using a previously described method (23).

Cellular Uptake. Cellular uptake experiments were also done using a previously published procedure (23).

Phototoxicity. Phototoxicity experiments were done using a previously published procedure (23). Preparation of cells and incubation conditions were essentially the same as those used in the cellular uptake experiments. Because some cell lines, notably NR6 cells, seemed to gradually efflux free BPD once the photosensitizer-laden culture media was replaced with fresh media, care was taken to irradiate cells immediately following replacement of the photosensitizer-laden culture media at the end of the incubation period. Cell viability was evaluated by colorimetric MTT (3-(4,5-dimethylthiazol-2-yl)-2,5-diphenyltetrazolium bromide) assay (30); this assay, which has frequently been used to assess chemo-, radio-, and phototoxic sensitivity, was used in this study rather than a clonogenic assay or other alternative nonclonogenic cell viability assay because it is fast and relatively easy to implement.

Competition Experiments. Competitions were done in both the cellular uptake and phototoxicity experiments. Binding of the BPD-C225 PICs to the EGFR was competed with varying amounts of either the native C225 MAb or a negative control antibody, Herceptin (anti-HER2 MAb). Experiments were conducted using saturating amounts of PIC coincubated with equal or greater concentrations of competing antibody.

SDS-PAGE Analysis of Cell-Mediated Photosensitizer Immunoconjugate Degradation. Cell lysate samples, each collected in 100 μL of lysis buffer [5 mmol/L disodium EDTA, 10 mmol/L Tris base, 150 mmol/L NaCl, 1% Triton X-100, 0.1% protease inhibitor cocktail solution (Sigma-Aldrich, St. Louis, MO), and 1 mmol/L phenylmethanesulfonyl fluoride; protease inhibitors were added just before use], were prepared from cells that had been incubated with PICs or free BPD using the same procedures as those used in the cellular uptake experiments. Based on protein content quantified by a Bradford-type protein assay (Bio-Rad Laboratories, Hercules, CA), equal amounts of each cell lysate sample were run on a 5% nonreducing SDS-PAGE gel. For comparison, a comparable amount of PIC stock solution was also run on the gel. Electrophoresis was done essentially by the method of Laemmli (31) using a SDS-discontinuous buffer system (Mini-PROTEAN II cell electrophoresis unit, Bio-Rad Laboratories). Gels were imaged and analyzed using a CCD camera gel-viewing system (ChemiImager, Alpha Innotech Corporation, San Leandro, CA) as previously described (23).

Photobleaching Quantum Yield Measurements. Photobleaching quantum yields were calculated as the number of moles of photodegraded BPD divided by the number of moles of photons absorbed. The initial BPD content of the sample solutions was roughly 10 μmol/L. For a control sample solution consisting of free BPD mixed with native C225 MAb, the antibody content was adjusted to equal that of the PIC sample solution. Samples were prepared in 50% DMSO/50% aqueous solutions, and measurements were conducted under air-saturated conditions. A 2.2 mL volume of sample solution was placed in a 1 cm pathlength cuvette and was irradiated with a 300 mW, 514 nm

argon ion laser source (model Innova 100; Coherent, Inc., Palo Alto, CA) while being stirred with a microstirring magnet. Absorption spectra of the sample solutions were measured after various irradiation times. The number of moles of photodegraded BPD was calculated for each sample solution by monitoring the loss of the 690 nm absorbance peak of BPD. For early time points, the 514 nm absorbance of the sample solutions did not significantly change relative to the loss in absorbance observed in the 690 nm peak. Therefore, to estimate the number of moles of photons absorbed by the samples, it was approximated that the rate of BPD absorbance of 514 nm photons was roughly constant.

Photodynamic Dose Calculations. Photodynamic dose calculations have usually ignored photobleaching to simplify analyses (10, 32–34). When photobleaching is ignored and a type II (singlet oxygen-mediated) photodynamic process is assumed, photodynamic dose can be roughly calculated using the following equation (10, 11):

$$[^1\triangle_g O_2]_{LD_{90}} = (J_{LD_{90}}\sigma\Phi_\triangle[PS]_0)/h\nu \qquad (A)$$

$[^1\Delta_g O_2]_{LD_{90}}$ is the number of singlet oxygen molecules generated per cell at LD_{90} (i.e., the dose that results in 90% cell killing), $J_{LD_{90}}$ is the LD_{90} light dose, σ is the photosensitizer absorption cross-section, Φ_Δ is the photosensitizer singlet oxygen quantum yield, $[PS]_0$ is the number of photosensitizer molecules bound per cell, and $h\nu$ is the excitation light photon energy. In more recent studies, photodynamic dose calculations have included the effects of photobleaching, which more accurately reflects the processes that occur in cellular environments during PDT (35, 36). When photobleaching occurs, the effective number of functional photosensitizer molecules decreases as the light dose, J, increases, and [PS] is a function of J:

$$[PS](J) = [PS]_0 \exp[(-\Phi_{PB}J\sigma)/h\nu] \qquad (B)$$

where Φ_{PB} is the photosensitizer photobleaching quantum yield. Consequently, when photobleaching is taken into account, Eq. A becomes the following:

$$[^1\triangle_g O_2]_{LD90} = \{(\Phi_\triangle[PS]_0)/\Phi_{PB}\} \times \{1 - \exp[(-\Phi_{PB}J_{LD90}\sigma)/h\nu]\} \qquad (C)$$

Eq. C was written somewhat ambiguously in previous reports. It should be evident that the argument in the exponential is explicitly negative. In this study, we accounted for photobleaching effects and used Eq. C to calculate photodynamic dose. Of course, if photobleaching is ignored and Eq. A is used instead, the calculated photodynamic dose is slightly higher (see ref. 11). Alternatively, Eqs. A or C, sans the factor Φ_Δ, yields the photodynamic dose expressed as the number of photons absorbed per cell.

RESULTS

Free Benzoporphyrin Derivative Phototoxicity Experiments. Although the free monoacid form of BPD has been shown to be a highly potent photosensitizer for PDT (15, 16), it exhibits no inherent specificity for malignant cells versus normal cells. To show that free BPD is nonspecific, and to establish a baseline for gauging the performance of the EGFR-targeted BPD-C225 PICs, free BPD phototoxicity experiments were conducted *in vitro* with two EGFR-overexpressing cell lines, A-431 and OVCAR-5; an EGFR-negative cell line, NR6; and a macrophage cell line, J774. Phototoxicity data were obtained for a range of free BPD concentrations and light doses (see ref. 11 for the comprehensive free BPD phototoxicity data set). Incubations were conducted for 40 hours at 37°C so that conditions would be comparable to those used in the PIC phototoxicity experiments for which prolonged incubations were necessary to attain appreciable cell killing. Although some variation in the free BPD photosensitivity of the various cell lines was observed, the phototoxicity experiments confirmed that free BPD is nonspecific. Greater than 90% cell killing (LD_{90}) was easily achieved for all cell lines using only moderate doses of free BPD and light. For example, at 140 nmol/L free BPD, LD_{90} light doses for A-431, OVCAR-5, NR6, and J774 cells were 3, 7 to 16 (depending on cell passage number), 9, and 2.5 J/cm^2, respectively.

Benzoporphyrin Derivative-C225 Photosensitizer Immunoconjugate Phototoxicity Experiments. To assess the specificity and potency of the EGFR-targeted BPD-C225 PICs, PIC phototoxicity experiments with target and nontarget cell lines were conducted *in vitro*. Figures 1 and 2 show a representative subset of the PIC phototoxicity data. PICs were incubated with the cells at a concentration of 140 or 280 nmol/L BPD content for 40 hours at 37°C, and light doses ranged from 0 up to 20 J/cm^2. PIC molar labeling ratios were ~7 or 10 BPD/antibody. Thus, the PIC incubation concentrations, in terms of C225 antibody content, ranged from about 14 up to 40 nmol/L. These PIC concentrations should have resulted in saturated binding of the PIC (as discussed later, BPD-C225 PIC binding affinity was estimated to be only slightly less than that of the native C225 MAb, which has a K_d of ~0.25 nmol/L; ref. 37). We chose to study PICs with 7 or 10 BPD/antibody in this investigation because PICs with <7 BPD/antibody were less phototoxic to target cells, and PICs with >11 BPD/antibody had notably lower binding affinity and were of poor purity (23).

The data show that the BPD-C225 PICs specifically targeted EGFR-overexpressing cells in the intended manner. Both EGFR-overexpressing cancer cell lines, A-431 and OVCAR-5, exhibited substantial decreases in viability after photoimmunotherapy treatment with the BPD-C225 PICs. OVCAR-5 cells were less responsive to EGFR-targeted photoimmunotherapy compared with A-431 cells (see Figs. 1*A, B*, and 2*A*), but gains in OVCAR-5 cell killing were achieved when the PIC molar labeling ratio was increased from 7 to 10 BPD/antibody. As expected, EGFR-negative NR6 cells were virtually unaffected when subjected to similar photoimmunotherapy treatment conditions. Cells that were treated with the PICs but not irradiated were also virtually unaffected.

Competitive Photoimmunotherapy Experiments. PIC specificity was shown by competition experiments between BPD-C225 PIC and 4- to 6-fold excess competing antibody. As shown in Fig. 1*A* and *B*, the phototoxic effect of the PIC was almost completely inhibited when competed with native C225.

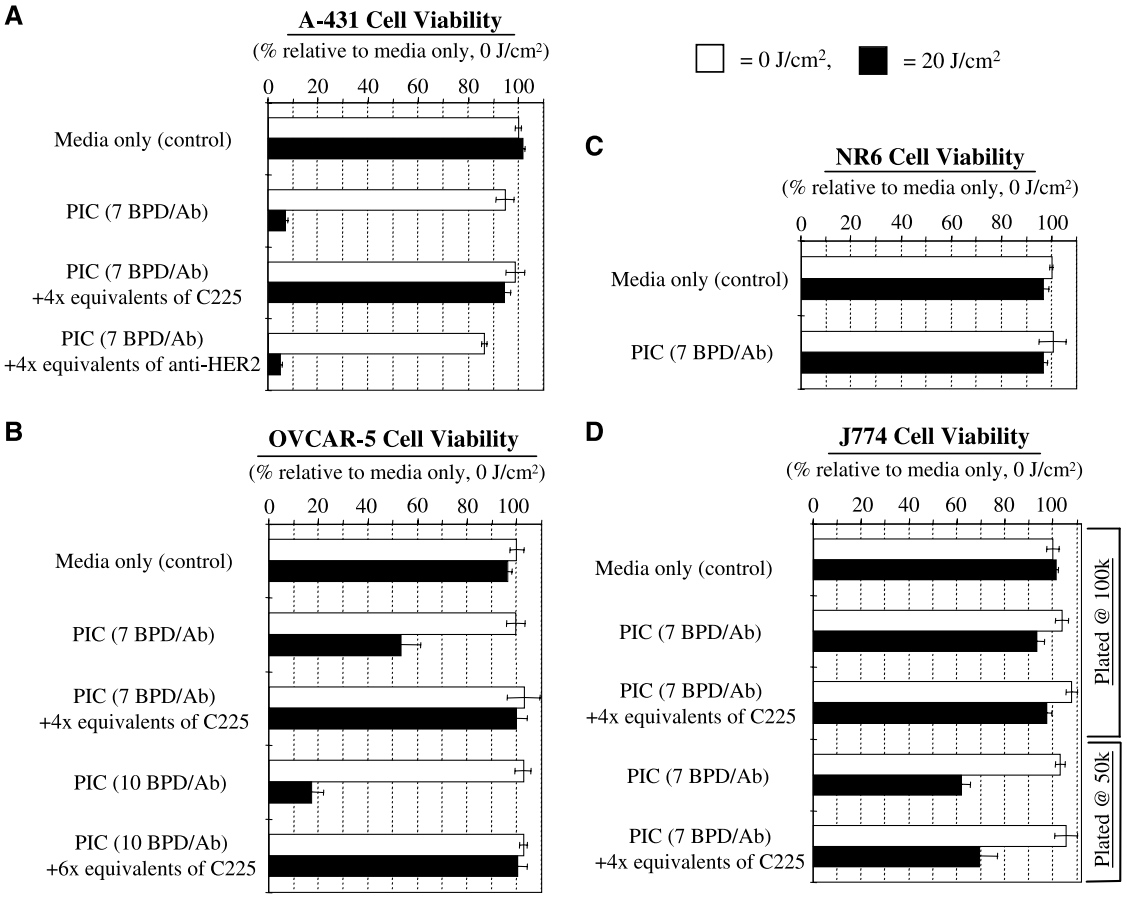

Fig. 1 Phototoxicity experiments with various cell lines demonstrating specificity and potency of the EGFR-targeted BPD-C225 PICs. *A,* A-431 cells (EGFR+); *B,* OVCAR-5 cells (EGFR+); *C,* NR6 cells (EGFR−); and *D,* J774 cells (macrophage). Cells were incubated for 40 hours at 37°C with PIC or, in some cases, PIC plus the indicated amount of competing antibody. The incubation concentration of PIC was 280 nmol/L BPD content (*A, C*, and *D*) or 140 nmol/L BPD content (*B*). Light doses were 0 J/cm^2 (*open horizontal columns*) and 20 J/cm^2 (*filled horizontal columns*). For J774 cell experiments (*D*), "Media only" data is not shown for initial plating densities of 50,000 cells per dish because this control data is essentially the same as that shown for initial plating densities of 100,000 cells per dish. All data were collected in triplicate; bars, SD.

No significant competition was observed when the competing antibody was Herceptin (Fig. 1*A*; refs. 38, 39), demonstrating exquisite selectivity. Herceptin targets the HER2/ErbB2 receptor, which is distinct from the EGFR but in the same ErbB receptor family.

Photoimmunotherapy treatment of the nontarget J774 macrophage cells with the BPD-C225 PIC resulted in a noticeable decrease in viability, which became more significant when the initial J774 cell plating density was decreased from 100,000 to 50,000 cells per 35 mm culture dish. Figure 1*D* shows that competition of the PIC with native C225 only minimally reduced J774 cell killing, regardless of the initial cell plating density. This suggests that photoimmunotherapy killing of J774 cells was *not* mediated by binding of the PIC to the EGFR but instead was most likely mediated by scavenger receptor-mediated endocytosis (40, 41) and/or nonspecific phagocytosis of small PIC aggregates. This explanation is also consistent with our previous work, which showed that polyethylene glycolation of the BPD-C225 PIC dramatically reduced aggregation and reduced the amount of PIC taken up by J774 cells (11, 23). However, our results indicate that even with polyethylene glycolation, some reticuloendothelial system capture of the BPD-C225 PIC may still be unavoidable *in vivo*.

Phototoxicity Experiments Comparing Free Benzoporphyrin Derivative with Benzoporphyrin Derivative-C225 Photosensitizer Immunoconjugates. In preliminary studies, we noted that the BPD-C225 PICs were less phototoxic than free BPD, even if the cells highly overexpressed the EGFR (11, 23). To investigate this matter in greater detail, phototoxicity experiments were conducted with EGFR-overexpressing A-431 cells, comparing free BPD with two different BPD-C225 PICs labeled with ~7 or ~10 BPD/antibody. Cells were incubated with PICs at 140 nmol/L BPD content or with free BPD at concentrations ranging from 14 up to 140 nmol/L. Incubations were done at 37°C for 40 hours, and light doses ranged from 0 to 20 J/cm^2. Figure 2*A* shows that the PIC with 10 BPD/antibody killed the A-431 cells more effectively than the PIC with 7 BPD/antibody, which correlates with the trend observed in similar experiments conducted with OVCAR-5 cells (see Fig. 1*B*). This was expected given that a PIC with a higher labeling ratio can deliver a larger photosensitizer payload per target receptor. However, Fig. 2*A* also shows that even at 5-fold lower concentration (28 nmol/L),

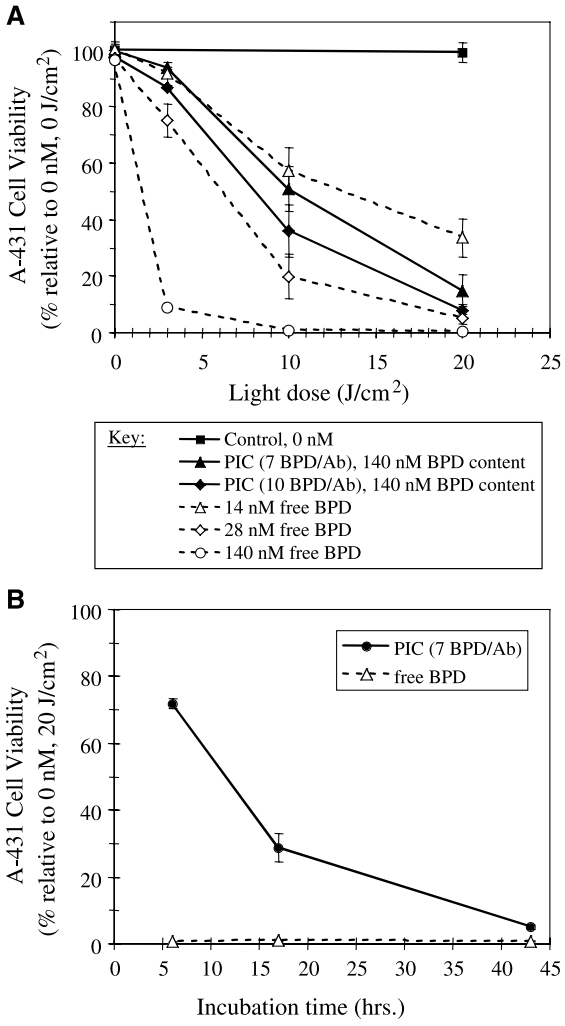

Fig. 2 Phototoxicity experiments with EGFR-overexpressing A-431 cells comparing free BPD with BPD-C225 PICs. *A,* cells were incubated with free BPD or BPD-C225 PICs (either 7 or 10 BPD/antibody) at the indicated concentrations for 40 hours at 37°C and then irradiated using a range of light doses; *B,* cells were incubated with free BPD or BPD-C225 PIC (7 BPD/antibody) at 280 nmol/L BPD content for various times at 37°C and then irradiated with a 20 J/cm^2 light dose. All data were collected in triplicate; bars, SD.

free BPD was more potent than either of the PICs. In fact, over the investigated light dose range, free BPD did not become notably less potent than the PICs until the incubation concentration was lowered to ~14 nmol/L.

Time-Coursed Incubation Phototoxicity Experiments Comparing Free Benzoporphyrin Derivative with Benzoporphyrin Derivative-C225 Photosensitizer Immunoconjugates. The time-coursed incubation phototoxicity experiments shown in Fig. 2*B* further show that formulation of BPD as a PIC radically changes its photochemical and photobiological properties. A431 cells were incubated with free BPD or BPD-C225 PIC (7 BPD/antibody) at 280 nmol/L BPD content for various times at 37°C and then irradiated with a 20 J/cm^2 light dose. As the incubation was prolonged from 6 to 43 hours, free BPD phototoxicity stayed roughly constant at ≥99% cell killing. Conversely, PIC phototoxicity gradually increased from ~30% cell killing at 6 hours to ≥90% cell killing at 43 hours but never reached the full phototoxic potency of free BPD over the investigated range of incubation times.

Cellular Uptake Experiments. Preliminary studies showed that the EGFR-targeted BPD-C225 PICs were taken up to a much greater extent by EGFR-overexpressing A-431 target cells than by EGFR-negative NR6 nontarget cells, although some nonspecific PIC uptake by J774 macrophage cells was observed (11, 23). In the present study, additional cellular uptake experiments were done to determine why OVCAR-5 target cells were less photosensitive than A-431 target cells to both free BPD and the BPD-C225 PICs and to determine why the PICs were less phototoxic than free BPD. We also wanted to estimate PIC binding affinity. Uptakes were measured as the number of femtomoles of BPD bound per cell.

Time-Coursed Incubation Cellular Uptake Experiments Comparing Free Benzoporphyrin Derivative with Benzoporphyrin Derivative-C225 Photosensitizer Immunoconjugate. Time-coursed incubation cellular uptake experiments are shown in Fig. 3*A*. Cells were incubated for various times at 37°C with 140 nmol/L BPD content of free BPD or BPD-C225 PIC (7 BPD/antibody). The two EGFR-positive target cell lines, A-431 and OVCAR-5, essentially exhibited similar uptake behavior. For both cell lines, initial free BPD and PIC uptake rates, although not directly measured, could be inferred to be much faster than the corresponding uptake rates observed at incubation times >5 hours. In addition, for both cell lines, the initial uptake of free BPD was greater than the initial uptake of PIC. However, following an initial period, the free BPD uptake no longer increased, whereas PIC uptake continued to increase gradually for both cell lines. For OVCAR-5 cells, free BPD uptake even seemed to drop slightly between 5 and 40 hours, suggesting that these cells may actively expel the free photosensitizer, perhaps via P-glycoprotein pump up-regulation (42). Taken as a whole, these results reflect the fact that free BPD is a hydrophobic and lipophilic small molecule that rapidly diffuses into hydrophobic cellular compartments, whereas the BPD-C225 PIC is a macromolecule that mainly enters target cells via a relatively slow process of receptor-mediated endocytosis involving the EGFR.

In terms of overall uptakes, A-431 cells took up more free BPD and more BPD-C225 PIC than OVCAR-5 cells. This most likely explains why A-431 cells were found to be more photosensitive than OVCAR-5 cells to both free BPD and BPD-C225 PICs. Assuming EGFR replenishment and recycling to the cell surface is probably negligible within the first few hours of incubation, we can estimate that the ratio of A-431 to OVCAR-5 uptake of the PIC, which is roughly 2.6 at the earliest time point examined (5 hours), is indicative of the relative EGFR expression levels of the two cell lines (11). It has been reported that A-431 cells express 1×10^6 to 2.6×10^6 EGFR per cell (24, 43). Therefore, one may estimate that OVCAR-5 cells express roughly 4×10^5 to 1×10^6 EGFR per cell. The different EGFR expression levels of the two target cell lines could largely explain why OVCAR-5 cells are less susceptible than A-431 cells to EGFR-targeted photoimmunotherapy.

For both target cell lines, the uptake of BPD-C225 PIC became comparable to or slightly greater than the uptake of free BPD for incubations ≥30 hours (see Fig. 3*A*). Consequently,

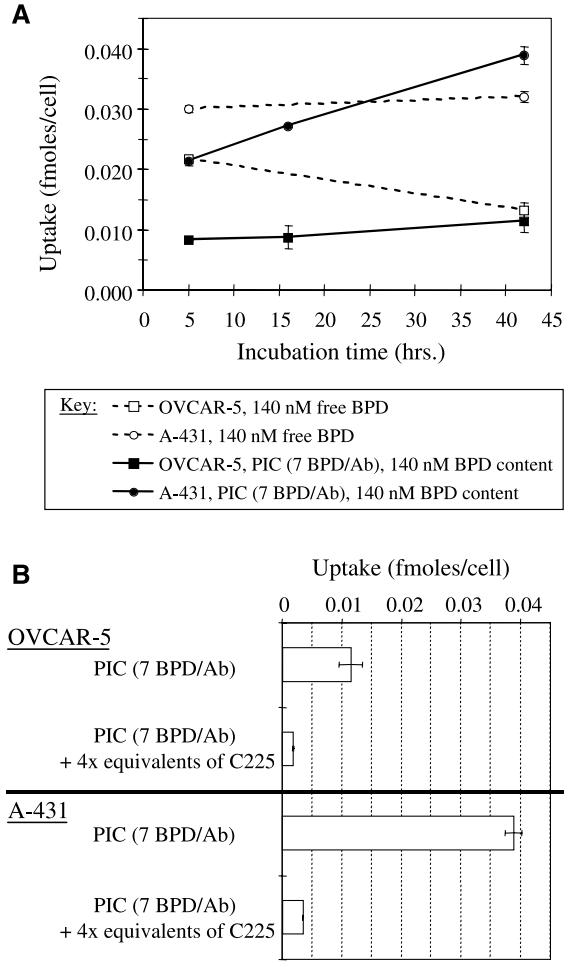

Fig. 3 Cellular uptake experiments with two EGFR-overexpressing cancer cell lines, OVCAR-5 and A-431. *A,* cells were incubated for various times at 37°C with 140 nmol/L BPD content of free BPD or BPD-C225 PIC; *B,* cells were incubated for ~40 hours at 37°C with 140 nmol/L BPD content of BPD-C225 PIC or BPD-C225 PIC plus the indicated amount of competing antibody. Data were collected in triplicate; bars, SD. Uptakes can be converted to femtomoles of BPD per milligram of cell protein using the following conversion factors: 2.4×10^6 cells/mg cell protein for OVCAR-5 and 1.8×10^6 cells/mg cell protein for A-431.

based solely on uptake measurements, one might predict for both target cell lines that PIC phototoxicity should be comparable to or exceed free BPD phototoxicity for incubations >30 hours. However, Fig. 2 clearly shows that for A-431 cells, PIC phototoxicity was still significantly less than free BPD phototoxicity for incubations >30 hours. The same trend holds for OVCAR-5 cells. Therefore, it must be concluded that cellular uptake levels alone cannot entirely explain why the BPD-C225 PICs are less phototoxic than free BPD to EGFR-overexpressing target cells.

Competitive Cellular Uptake Experiments. Competitive cellular uptake experiments, pitting BPD-C225 PIC against native C225, are shown in Fig. 3*B*. Cells were incubated for ~40 hours at 37°C with 140 nmol/L BPD content of BPD-C225 PIC (7 BPD/antibody) or BPD-C225 PIC plus the indicated amount of competing antibody. Assuming that PIC binding affinity is roughly the same as that of native C225 and that binding is saturated, roughly 80% inhibition would be expected in the competitive uptake experiments [80 nmol/L of C225 MAb / (20 nmol/L C225 MAb content of PIC + 80 nmol/L of C225 MAb) = 80%]. In fact, the observed inhibition of PIC uptake for both target cell lines was somewhat >80%. For OVCAR-5 cells, the competed uptake was ~15% of the uncompeted uptake or, in other words, PIC uptake was inhibited by ~85%. Similarly, for A-431 cells, PIC uptake was inhibited by ~90%. This suggests that the BPD-C225 PIC binding affinity is somewhat less than the native C225 MAb binding affinity.

Using the results of the competitive cellular uptake experiments, BPD-C225 PIC binding affinity can be estimated to be about two times less than that of the native C225 MAb; i.e., the K_d for the BPD-C225 PIC with a labeling ratio of 7 BPD/antibody can be estimated to be ~0.5 nmol/L. This estimate is valid provided the PIC does not contain a significant amount of noncovalently associated free BPD impurity. We have shown that our PIC preparations are of high purity, so we believe that the estimated K_d for the BPD-C225 PIC is fairly reasonable, although strictly speaking, it can only serve as a lower-bound estimate (11). The estimate of PIC binding affinity is based on competitive uptake experiments that were done only for the PIC with ~7 BPD/antibody. It should be pointed out that PIC binding affinity most likely depends on the degree of PIC loading, decreasing as the BPD/antibody molar ratio of the PIC increases.

Cell-Mediated Photosensitizer Immunoconjugate Degradation Experiments. In addition to cellular uptakes, other factors had to be considered to ascertain why the BPD-C225 PICs gradually increased in potency but never actually reached the full phototoxic potency of free BPD as incubation periods were prolonged up to ~40 hours. Prior to incubation with target cells, the BPD-C225 PICs are fully intact and are photophysically quenched due to static concentration quenching effects (11, 23). Consequently, we hypothesized that as incubation times increased, the BPD-C225 PICs could have gradually degraded in the lysosomes of target cells, thereby releasing photosensitizer from the PIC in a more photoactive form, either as free BPD or as degraded PIC fragments. Lysosomal degradation of the PIC also could have resulted in redistribution of the photosensitizer to other more critically photosensitive subcellular sites.

To assess the degree of BPD-C225 PIC catabolism as a function of incubation time, we conducted cell-mediated PIC degradation experiments with the A-431 target cells. Figure 4 shows a fluorescent SDS-PAGE gel image of various A-431 cell lysates prepared from time-coursed incubations with free BPD or BPD-C225 PIC. Unbound PIC or unbound free BPD was washed away before collecting cell lysates to ensure the lysates only contained PIC or free BPD that had been taken up and bound by the cells. As expected, PIC breakdown increased as incubations were prolonged. This was deduced from Fig. 4 by noting that as incubation times increased, the PIC fluorescence in region R1 gradually decreased, whereas the PIC fluorescence in region R2 gradually increased. The fraction of intact PIC remaining at different incubation times could be quantified by comparing the amounts of fluorescence running in the two regions. At 1, 4, 17, and 40 hours, the fraction of intact PIC was 0.97, 0.86, 0.63, and 0.55, respectively. In contrast, for cells that

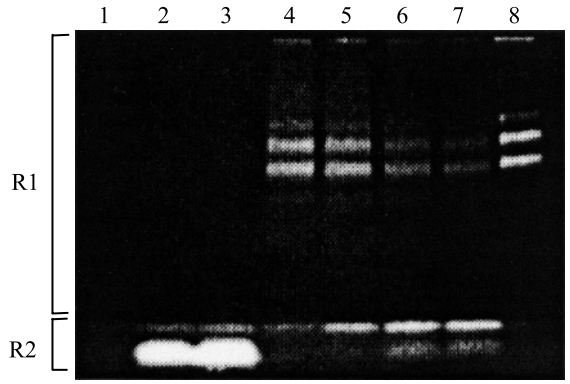

Fig. 4 SDS-PAGE analysis (5% nonreducing gel) of A-431 cell lysates prepared from time-coursed incubations with free BPD or BPD-C225 PIC. The photosensitizer fluorescence of the gel was imaged as described in Materials and Methods. Cell lysates were prepared by incubating cells for various times at 37°C with 280 nmol/L BPD content of free BPD or PIC (7 BPD/antibody). Intact PIC runs in region R1, and broken down PIC or free BPD runs in region R2. (*Lane 1*) cells incubated with media only, (*lane 2*) cells incubated for 1 hour with free BPD, (*lane 3*) cells incubated for 40 hours with free BPD, (*lane 4*) cells incubated for 1 hour with PIC, (*lane 5*) cells incubated for 4 hours with PIC, (*lane 6*) cells incubated for 17 hours with PIC, (*lane 7*) cells incubated for 40 hours with PIC, and (*lane 8*) 0.5 μL of the original 30 μmol/L (BPD content) stock solution of PIC.

were incubated with free BPD, virtually all of the BPD fluorescence ran in region R2 and very little ran in region R1, regardless of the length of the incubation period.

For the 5% nonreducing SDS-PAGE gels of these studies, we have shown that intact PIC consists of three major bands running in region R1 at roughly 170, 179, and 198 kDa, and that the interface of regions R1 and R2 roughly corresponds to a 47 kDa ovalbumin standard (11, 23). Figure 4 shows that the majority of the degraded PIC is most likely significantly larger than free BPD (~719 Da). In fact, in confocal microscopy studies, we have observed that the PICs predominantly localize in endosomes and/or lysosomes and do not redistribute to other subcellular sites over time (11, 22),[4] suggesting that PIC degradation fragments are too large to escape the endosomes and/or lysosomes.

Estimating Photophysical and Photochemical Parameters. To calculate photodynamic doses, several photophysical and photochemical parameters had to be estimated. Table 1 gives the photon energy of the excitation light ($h\nu$), absorbance cross-sections (σ), singlet oxygen quantum yields (Φ_Δ), and photobleaching quantum yields (Φ_{PB}) for free BPD and two different BPD-C225 PICs with labeling ratios of ~7 or ~10 BPD/antibody. Parameters were cautiously estimated assuming 40-hour incubations at 37°C with target cells, and photodynamic dose calculations presented herein should be regarded as upper-bound estimates.

For all phototoxicity experiments, the wavelength of the laser excitation light, λ, was ~690 nm, and the corresponding photon energy, $h\nu$, was simply calculated as hc/λ, where h is Planck's constant and c is the speed of light. Because the 690 nm absorbance cross-section, σ, for free BPD and for the BPD-C225 PICs in heterogeneous cellular environments could not be directly measured, it was estimated to be equal to that of free BPD in DMSO, $\sim 1.395 \times 10^{-16}$ cm^2. For free BPD in cells, this σ value seems to be fairly reasonable, given that free BPD is generally thought to be well solubilized and predominantly disaggregated within the hydrophobic compartments of cells, which is similar to the behavior of free BPD in DMSO. However, for the BPD-C225 PICs, this σ value may be slightly overestimated, given that the PIC absorbance spectra in homogeneous solutions are characteristic of aggregated BPD (11, 23). Based on detailed aggregation studies (12), we believe that our approximated σ value for the BPD-C225 PICs is at most overestimated by a factor of 2 or 3. Although a method for measuring the extinction coefficient of a photosensitizer conjugate has been described (32), we did not attempt to use the method to obtain more precise σ values of the PICs due to the technical challenges involved. Moreover, we are aware that cellular degradation of the PICs during prolonged incubations could have resulted in a gradual increase in their effective absorbance cross-sections over time.

Accurately measuring the singlet oxygen quantum yield, Φ_Δ, of a photosensitizer in heterogeneous cellular environments is extremely difficult (44, 45). Therefore, Φ_Δ for free BPD in cells was estimated to be equal to that of free BPD in homogeneous organic solvents, ~0.77 (16). Again, this approximation is reasonable because free BPD seems to be well-solubilized and predominantly disaggregated (i.e., monomeric) within the hydrophobic compartments of cells, which is similar to the behavior of free BPD in homogeneous organic solvents.

Estimating Φ_Δ for the BPD-C225 PICs in cells involved a more complex analysis. First, it was assumed that PIC fluorescence static concentration quenching, which had been assessed quantitatively in an earlier study (11, 23), reflected the degree of quenching of PIC singlet oxygen production. This seems to be a fair assumption because Φ_Δ is usually proportional to the photosensitizer triplet quantum yield, Φ_T, and Φ_T is typically proportional to the photosensitizer excited singlet state lifetime, τ_S. [For BPD, Φ_T tracks with the fluorescence quantum yield as photosensitizer aggregation state is varied (ref. 12), suggesting that static concentration quenching does not disrupt the proportionality relationship between Φ_T and τ_S. In general, Φ_Δ, Φ_T, and τ_S are usually all proportional to one another, but

Table 1 Estimates of various photophysical and photochemical parameters used in calculating photodynamic doses, assuming 40-hour incubations with cells at 37°C

Photosensitizer or PIC	$h\nu$ (690 nm), J	σ (690 nm), cm^2	Φ_Δ	Φ_{PB}
Free BPD	2.879×10^{-19}	1.395×10^{-16}	0.77	9.2×10^{-5}
PIC (7 BPD/antibody)	2.879×10^{-19}	1.395×10^{-16}	0.411	5.93×10^{-5}
PIC (10 BPD/antibody)	2.879×10^{-19}	1.395×10^{-16}	0.394	5.93×10^{-5}

it should be noted that Φ_Δ is also affected by photosensitizer intersystem crossing and triplet relaxation rates.] Second, based on the cell-mediated PIC degradation studies, we estimated that ~45% of the PIC had broken down into fragments, perhaps as small as free BPD, and that ~55% of the PIC still remained intact after 40-hour incubations with the target cells at 37°C. Consequently, for the 7 BPD/antibody PIC, Φ_Δ was approximated as $(0.45) \times (0.77) + (0.55) \times (0.152) \times (0.77) \approx 0.411$, where 0.45 and 0.55 are the respective fractions of degraded and intact PIC, 0.77 is the Φ_Δ value for monomeric free BPD, and 0.152 is the relative fluorescence quantum yield of the PIC compared with monomeric free BPD (11, 23). For the 10 BPD/antibody PIC, Φ_Δ was similarly estimated to be ~0.394.

Photobleaching quantum yields for free BPD and the BPD-C225 PICs also could not be reliably measured in heterogeneous cellular environments. Instead, they were measured in a homogenous 50% DMSO/50% aqueous two-solvent system under air-saturated conditions. Free BPD is well solubilized and predominantly monomeric in this two-solvent system, which is probably similar to its solubility behavior in cells. Moreover, the PIC remains quenched and nondenatured but does not seem to be significantly aggregated in the two-solvent system, which seems to be the case for intact noncatabolized PIC in cellular environments. Measured photobleaching quantum yields were 9.2×10^{-5}, 6.7×10^{-5}, and 2.2×10^{-5} to 4.3×10^{-5} for free BPD, free BPD plus native C225 MAb, and PIC (7 BPD/antibody), respectively. The Φ_{PB} value of the PIC is expressed as a range because the PIC extinction coefficient could not be precisely measured, as discussed earlier. To simplify subsequent analyses, Φ_{PB} for both the 7 and 10 BPD/antibody PICs was approximated as the median of this range (3.25×10^{-5}). The fact that the free BPD plus native C225 MAb sample has an intermediate Φ_{PB} value between that of free BPD and the PIC indicates that static concentration quenching suppresses the PIC photobleaching quantum yield to a greater degree than what can be expected due solely to the presence of the MAb.

Based on arguments similar to those used to estimate Φ_Δ in cells, Φ_{PB} for the PICs in cellular environments was extrapolated roughly as $(0.45) \times (9.2 \times 10^{-5}) + (0.55) \times (3.25 \times 10^{-5}) \approx 5.93 \times 10^{-5}$. The factors 0.45 and 0.55 are the respective fractions of degraded and intact PIC after 40-hour incubations with target cells at 37°C, and the factors 9.2×10^{-5} and 3.25×10^{-5} are the Φ_{PB} values measured for free BPD and intact PIC, respectively. Our measured Φ_{PB} value for free BPD, which we assume is also roughly equal to the Φ_{PB} values of the cell-degraded PIC fragments, is slightly lower than previously reported values (16). Therefore, Φ_{PB} values in this present study should probably be considered lower bound estimates. By way of comparison, in a study of two chlorin-type photosensitizers, photobleaching was much greater for cell-bound photosensitizer than for photosensitizer solubilized in homogenous solutions (35). However, for free BPD in a wide variety of media, Φ_{PB} was always found to lie in a relatively narrow range between $\sim 10^{-5}$ and $\sim 10^{-4}$ (16), suggesting that our measured and extrapolated Φ_{PB} values are at least the right order of magnitude.

Photodynamic Dose Calculations. Table 2 shows the calculated LD_{90} doses for various experiments with the EGFR-overexpressing target cell lines, A-431 and OVCAR-5. Cells were incubated with 140 nmol/L BPD content of free BPD or BPD-C225 PIC (~7 or ~10 BPD/antibody) for 40 hours at 37°C, and then cellular uptake and phototoxicity experiments were conducted. The most definitive measure of photodynamic dosage is the calculated number of photons absorbed per cell, because no assumptions are made about the nature of the phototoxic species. However, because it is often fair to assume that the primary phototoxic species is singlet oxygen, $^1\Delta_g O_2$ (46), we also report dosage as the calculated number of $^1\Delta_g O_2$ molecules generated per cell.

For both target cell lines, the LD_{90} light dose ($J_{LD_{90}}$) for free BPD was substantially lower than the LD_{90} light doses for the BPD-C225 PICs, although PIC uptakes were comparable to or slightly greater than free BPD uptakes (see Table 2). If differences in photobleaching quantum yields are taken into account, the calculated LD_{90} doses for the PICs, expressed as the number of photons absorbed per cell, are significantly higher than those for free BPD. Moreover, if differences in photobleaching and singlet oxygen quantum yields are both taken into account, the calculated LD_{90} doses for the PICs, expressed as the number of $^1\Delta_g O_2$ molecules generated per cell, are still somewhat higher than those for free BPD. Taken as a whole, these results suggest that in addition to uptake levels, photobleaching, and singlet oxygen quantum yields, other factors also must have adversely affected the phototoxic potency of the PICs.

Table 2 Calculated LD_{90} photodynamic doses based on cellular uptake and phototoxicity experiments with the EGFR-overexpressing target cell lines, A-431 and OVCAR-5

Experiment	Uptake, $[PS]_0$, molecules of BPD per cell	$[PS]_{LD_{90}}/[PS]_0$, fraction of non-photobleached BPD molecules at LD_{90}	LD_{90} light dose, $J_{LD_{90}}$, J/cm_2	Number of photons absorbed per cell at LD_{90}	Number of $^1\Delta_g O_2$ generated per cell at LD_{90}
A-431 cells					
Free BPD	1.9×10^7	0.87	3	2.59×10^{10}	1.99×10^{10}
PIC (7 BPD/antibody)	2.3×10^7	0.55	21	1.76×10^{11}	7.22×10^{10}
PIC (10 BPD/antibody)	3.3×10^7	0.58	19	2.34×10^{11}	9.21×10^{10}
OVCAR-5 cells					
Free BPD	8.0×10^6	0.73	7	2.33×10^{10}	1.79×10^{10}
PIC (7 BPD/antibody)	6.9×10^6	0.15	65	9.84×10^{10}	4.04×10^{10}
PIC (10 BPD/antibody)	9.9×10^6	0.53	22	7.82×10^{10}	3.08×10^{10}

NOTE. Cells were incubated with 140 nmol/L BPD content of free BPD or PIC for 40 hours at 37°C.

Finally, we examined how photobleaching impacted the overall capacity to generate an effective photodynamic dose. Table 2 shows that the calculated photosensitizer cellular concentration at LD_{90}, $[PS]_{LD_{90}}$, was always ≥50% of the total photosensitizer cellular uptake, $[PS]_0$, in all the experiments except photoimmunotherapy treatment of OVCAR-5 cells with the 7 BPD/antibody PIC. Therefore, in all experiments except photoimmunotherapy treatment of OVCAR-5 cells with the 7 BPD/antibody PIC, reaching and exceeding LD_{90} does not seem to have been appreciably hindered by photobleaching. However, only about 15% of the total photosensitizer cellular uptake effectively remained at LD_{90} for photoimmunotherapy treatment of OVCAR-5 cells with the 7 BPD/antibody PIC. In this case, it seems that photobleaching significantly impeded the attainment of an LD_{90} dose. This seems to explain why $J_{LD_{90}}$ for photoimmunotherapy treatment of OVCAR-5 cells with the 7 BPD/antibody PIC was at least three times greater than $J_{LD_{90}}$ for all the other phototoxicity experiments. Of course, these results also correlate with the earlier observation that OVCAR-5 cells express fewer EGFR than A-431 cells.

DISCUSSION

The BPD-C225 PICs selectively targeted and photodynamically killed EGFR-overexpressing cancer cells, whereas free BPD exhibited no specificity. On a per molecule basis, the PICs were substantially less phototoxic than free BPD. As incubation periods were prolonged, PIC phototoxicity gradually increased, presumably due to increased cellular uptake, internalization, degradation, and dequenching of the PICs. Even so, after incubations as long as 40 hours, BPD-C225 PICs were still less phototoxic than free BPD. To explain these findings, we did photodynamic dose calculations to analyze our experimental results. We found that uptake levels alone could not explain why the PICs were significantly less phototoxic than free BPD. Moreover, even after accounting for PIC cellular degradation and dequenching, we found that differences in the photobleaching and singlet oxygen quantum yields between the PICs and free BPD still could not entirely explain why the PICs were less phototoxic than free BPD. The relatively lower phototoxic efficacy of the PICs is not a serious problem in terms of therapeutic viability as both light and PIC doses may be increased provided the PICs remain selective. The critical issue in cancer therapy is selectivity. Almost all PDT agents and cytotoxic drugs are effective against cancer cells at some concentration. However, their use is limited by their toxicity to normal cells and tissues at higher, therapeutically effective concentrations. With selective therapy, doses may be increased to a greater extent to achieve effective destruction.

Subcellular localization may have been an additional contributing factor that adversely affected the phototoxic potency of the BPD-C225 PICs. We have previously noted that the cellular fluorescence of the BPD-C225 PICs gradually increases over time and predominantly localizes in the endosomes and/or lysosomes of target cells, whereas the cellular fluorescence of free BPD does not change appreciably over time and diffusely stains membranous structures, especially the perinuclear region of cells (11, 22). The observed subcellular localization of the BPD-C225 PICs supports the hypothesis that they enter target cells via receptor-mediated endocytosis involving the EGFR and then undergo sorting to the endosomes and lysosomes where they are eventually degraded (a small fraction of PIC might also enter cells via nonspecific fluid phase and/or adsorptive pinocytosis). On the other hand, the observed subcellular localization of free BPD is consistent with the fact that it is a small hydrophobic/lipophilic molecule that rapidly sequesters in the hydrophobic compartments of cells. One important subcellular site to which free BPD localizes are the mitochondria. Mitochondria are highly photosensitive, and this correlates with the induction of rapid apoptosis following PDT with free BPD (47–49). Conversely, lysosomes seem to be less photosensitive than mitochondria in terms of inducing rapid apoptosis (50–53).

The reduced phototoxicity of the PIC compared with the free photosensitizer highlights an inherent trade-off between selectivity and potency. Our view is that for treatment of cancer and other pathologies, selectivity is currently the major limitation; many potent drugs are available, but toxic side effects often limit their use. To improve the efficacy of photoimmunotherapy and still maintain selectivity, one could simply apply a higher light dose, provided photobleaching is not a limiting factor. Another possibility is to further extend the incubation period to allow more extensive lysosomal breakdown of the PIC, which could yield more optimal dequenching of the PIC and permit photosensitizer redistribution from the endosomes and lysosomes to other more critically photosensitive subcellular sites. PIC degradation could also be further enhanced by incorporating lysosomal enzyme-cleavable linkers (54, 55) between the MAb and photosensitizer.

Target receptor expression levels and target receptor internalization/turnover rates are critical parameters in photoimmunotherapy. EGFR expression levels were $\sim 5 \times 10^5$ to $\sim 2.5 \times 10^6$ per cell for the target cell lines in this study, and the BPD/antibody molar ratios of the BPD-C225 PICs were as high as ~10, implying that the PICs could deliver $\gtrsim 5 \times 10^6$ BPD molecules per cell. Phototoxicity experiments indicated that photobleaching did not appreciably hinder the attainment of LD ≥90, provided the photosensitizer uptake levels were significantly greater than $\sim 5 \times 10^6$ BPD molecules per cell. Thus, it can be inferred that target cells possessing less than $\sim 5 \times 10^5$ EGFR per cell most likely will be difficult to kill with the BPD-C225 PICs. By the same token, nontarget cells possessing significantly less than $\sim 5 \times 10^5$ EGFR per cell should be spared (nonmalignant cells in culture typically express $\leq 10^4$ EGFR per cell; ref. 24).

We have found that it is difficult to make PICs with BPD/antibody molar ratios >11 without sacrificing PIC binding affinity and purity (23). To boost PIC uptake levels without having to achieve further increases in photosensitizer-antibody labeling ratios, multitargeting strategies could be implemented using a combination of different PICs to target multiple epitopes on the same receptor and/or multiple epitopes on different receptors. In fact, targeting multiple ErbB2 receptor epitopes using a cocktail of three different anti-ErbB2 MAbs has been shown to be feasible and more effective than single MAb anti-ErbB2 therapy (56). Targeting more than one type of receptor with a mixture of PICs could also result in synergistic therapeutic

effects. For example, combined anti-EGFR MAb/antivascular endothelial growth factor-receptor-2 MAb therapy has been shown to be more effective than the single MAb therapies (57).

Many groups, including our own, have shown the possibilities of photoimmunotherapy, but there has been no in-depth analysis of the dosimetric and mechanistic aspects of photoimmunotherapy. We believe that this is the first *in vitro* study to delineate the complex processes and mechanisms involved in EGFR-targeted photoimmunotherapy. The results suggest that receptor-targeted photoimmunotherapy warrants further investigation. As a next step, the PICs will be tested in appropriate *in vivo* models, where the additional complexities of physiologic barriers (58, 59) will be encountered. Insights gained from this detailed *in vitro* study should allow a clearer interpretation and better understanding of future *in vivo* photoimmunotherapy studies.

ACKNOWLEDGMENTS

We thank Drs. Robert Gilmont, Riley Rees, and Stephen Rand, who helped initiate this work; Krishnan Rajagopalan and Richard Lawton, who provided guidance with synthesis and purification issues; Robert Redmond, who provided advice regarding photophysical and photochemical measurements; and Michael Hamblin for challenging discussions.

REFERENCES

1. Hasan T, Ortel B, Moor A, Pogue B. Photodynamic therapy of cancer. In: Kufe, Pollock, Weichselbaum et al, editors. Cancer Medicine, 6th ed. Hamilton, Ontario (B.C.): Decker, Inc; 2003. p. 605–22.

2. Mew D, Wat CK, Towers GH, Levy JG. Photoimmunotherapy: treatment of animal tumors with tumor-specific monoclonal antibody-hematoporphyrin conjugates. J Immunol 1983;130:1473–7.

3. Mendelsohn J, Fan Z. Epidermal growth factor receptor family and chemosensitization. J Natl Cancer Inst 1997;89:341–3.

4. Harari PM, Huang SM. Head and neck cancer as a clinical model for molecular targeting of therapy: combining EGFR blockade with radiation. Int J Radiat Oncol Biol Phys 2001;49:427–33.

5. de Bono JS, Rowinsky EK. The ErbB receptor family: a therapeutic target for cancer. Trends Mol Med 2002;8:S19–26.

6. Soukos NS, Hamblin MR, Keel S, Fabian RL, Deutsch TF, Hasan T. Epidermal growth factor receptor-targeted immunophotodiagnosis and photoimmunotherapy of oral precancer *in vivo*. Cancer Res 2001;61: 4490–6.

7. Schmidt S, Wagner U, Oehr P, Krebs D. Clinical use of photodynamic therapy in gynecologic tumor patients—antibody-targeted photodynamic laser therapy as a new oncologic treatment procedure. Zentralbl Gynakol 1992;114:307–11.

8. Hasan T. Photosensitizer delivery mediated by macromolecular carrier systems. In: Henderson BW, Dougherty TJ, editors. Photodynamic therapy: basic principles and clinical applications, New York: Marcel Dekker, Inc; 1992. p. 187–200.

9. Sternberg ED, Dolphin D, Brückner C. Porphyrin-based photosensitizers for use in photodynamic therapy. Tetrahedron 1998;54: 4151–202.

10. Yarmush ML, Thorpe WP, Strong L, Rakestraw SL, Toner M, Tompkins RG. Antibody targeted photolysis. Crit Rev Ther Drug Carrier Syst 1993;10:197–252.

11. Savellano MD. Photodynamic targeting with photosensitizer immunoconjugates. Ph.D. Thesis. Ann Arbor, MI: Department of Biomedical Engineering, University of Michigan; available online from UMI Dissertations Publishing; 2000.

12. Aveline BM, Hasan T, Redmond RW. The effects of aggregation, protein binding and cellular incorporation on the photophysical properties of benzoporphyrin derivative monoacid ring A (BPDMA). J Photochem Photobiol B 1995;30:161–9.

13. Vrouenraets MB, Visser GW, Stewart FA, et al. Development of meta-tetrahydroxyphenylchlorin-monoclonal antibody conjugates for photoimmunotherapy. Cancer Res 1999;59:1505–13.

14. Vrouenraets MB, Visser GW, Stigter M, Oppelaar H, Snow GB, van Dongen GA. Targeting of aluminum (III) phthalocyanine tetrasulfonate by use of internalizing monoclonal antibodies: improved efficacy in photodynamic therapy. Cancer Res 2001;61:1970–5.

15. Richter AM, Kelly B, Chow J, et al. Preliminary studies on a more effective phototoxic agent than hematoporphyrin. J Natl Cancer Inst 1987;79:1327–32.

16. Aveline B, Hasan T, Redmond RW. Photophysical and photosensitizing properties of benzoporphyrin derivative monoacid ring A (BPD-MA). Photochem Photobiol 1994;59:328–35.

17. Levy JG, Dolphin D, Chow JK. Wavelength-specific cytotoxic agents, U.S. patent: 4,883,790. 1989.

18. Jiang FN, Jiang S, Liu D, Richter A, Levy JG. Development of technology for linking photosensitizers to a model monoclonal antibody. J Immunol Methods 1990;134:139–49.

19. Jiang FN, Liu DJ, Neyndorff H, Chester M, Jiang SY, Levy JG. Photodynamic killing of human squamous cell carcinoma cells using a monoclonal antibody-photosensitizer conjugate. J Natl Cancer Inst 1991; 83:1218–25.

20. Jiang FN, Allison B, Liu D, Levy JG. Enhanced photodynamic killing of target cells by either monoclonal antibody or low density lipoprotein mediated delivery systems. J Control Release 1992;19: 41–58.

21. Jiang FN, Richter AM, Jain AK, Levy JG, Smits C. Biodistribution of a benzoporphyrin derivative-monoclonal antibody conjugate in A549-tumor-bearing nude mice. Biotechnol Ther 1993;4:43–61.

22. Savellano MD, Rand SC, Hasan T. PEGylated BPD Verteporfin C225 anti-EGF receptor direct covalent linkage photosensitizer immunoconjugates. Photochem Photobiol 1999;69S:38S.

23. Savellano MD, Hasan T. Targeting cells that overexpress the epidermal growth factor receptor with polyethylene glycolated BPD verteporfin photosensitizer immunoconjugates. Photochem Photobiol 2003;77:431–9.

24. Mendelsohn J. Epidermal growth factor receptor inhibition by a monoclonal antibody as anticancer therapy. Clin Cancer Res 1997;3: 2703–7.

25. Fan Z, Mendelsohn J. Therapeutic application of anti-growth factor receptor antibodies. Curr Opin Oncol 1998;10:67–73.

26. Garber K. New discoveries still abundant in monoclonal antibody research. J Natl Cancer Inst 2000;92:1462–4.

27. Perkins AS, Stern DF. In: DeVita VT, Hellman S, Rosenberg SA, editors. Cancer: principles and practice of oncology. Philadelphia: Lippincott-Raven; 1997. p. 79–102.

28. Schmidt-Erfurth U, Hasan T. Mechanisms of action of photodynamic therapy with verteporfin for the treatment of age-related macular degeneration. Surv Ophthalmol 2000;45:195–214.

29. Pruss RM, Herschman HR. Variants of 3T3 cells lacking mitogenic response to epidermal growth factor. Proc Natl Acad Sci U S A 1977;74: 3918–21.

30. Mosmann T. Rapid colorimetric assay for cellular growth and survival: application to proliferation and cytotoxicity assays. J Immunol Methods 1983;65:55–63.

31. Laemmli UK. Cleavage of structural proteins during the assembly of the head of bacteriophage T4. Nature 1970;227:680–5.

32. Rakestraw SL, Ford WE, Tompkins RG, Rodgers MA, Thorpe WP, Yarmush ML. Antibody-targeted photolysis: *in vitro* immunological, photophysical, and cytotoxic properties of monoclonal antibody-dextran-Sn(IV) chlorin e6 immunoconjugates. Biotechnol Prog 1992;8:30–9.

33. Oseroff AR, Ohuoha D, Hasan T, Bommer JC, Yarmush ML. Antibody-targeted photolysis: selective photodestruction of human T-cell leukemia cells using monoclonal antibody-chlorin e6 conjugates. Proc Natl Acad Sci U S A 1986;83:8744–8.

34. Gross S, Brandis A, Chen L, et al. Protein-A-mediated targeting of bacteriochlorophyll-IgG to *Staphylococcus aureus*: a model for enhanced site-specific photocytotoxicity. Photochem Photobiol 1997;66:872–8.

35. Pogue BW, Ortel B, Chen N, Redmond RW, Hasan T. A photobiological and photophysical-based study of phototoxicity of two chlorins. Cancer Res 2001;61:717–24.

36. Pogue BW, Redmond RW, Trivedi N, Hasan T. Photophysical properties of tin ethyl etiopurpurin I (SnET2) and tin octaethylbenzochlorin (SnOEBC) in solution and bound to albumin. Photochem Photobiol 1998;68:809–15.

37. Goldstein NI, Prewett M, Zuklys K, Rockwell P, Mendelsohn J. Biological efficacy of a chimeric antibody to the epidermal growth factor receptor in a human tumor xenograft model. Clin Cancer Res 1995;1: 1311–8.

38. Shak S. Overview of the trastuzumab (Herceptin) anti-HER2 monoclonal antibody clinical program in HER2-overexpressing metastatic breast cancer. Herceptin Multinational Investigator Study Group. Semin Oncol 1999;26:71–7.

39. Ye D, Mendelsohn J, Fan Z. Augmentation of a humanized anti-HER2 mAb 4D5 induced growth inhibition by a human-mouse chimeric anti-EGF receptor mAb C225. Oncogene 1999;18:731–8.

40. Hamblin MR, Penta P, Ortel B, Hasan T. Targeting phototoxicity to macrophages via albumin photosensitizer conjugates. Photochem Photobiol 1998;67S:92S.

41. Brasseur N, Langlois R, La Madeleine C, Ouellet R, van Lier JE. Receptor-mediated targeting of phthalocyanines to macrophages via covalent coupling to native or maleylated bovine serum albumin. Photochem Photobiol 1999;69:345–52.

42. Pastan I, Gottesman M. Multiple-drug resistance in human cancer. N Engl J Med 1987;316:1388–93.

43. Haigler H, Ash JF, Singer SJ, Cohen S. Visualization by fluorescence of the binding and internalization of epidermal growth factor in human carcinoma cells A-431. Proc Natl Acad Sci U S A 1978; 75:3317–21.

44. Gorman AA, Rodgers MA. Current perspectives of singlet oxygen detection in biological environments. J Photochem Photobiol B 1992;14: 159–76.

45. Niedre M, Patterson MS, Wilson BC. Direct near-infrared luminescence detection of singlet oxygen generated by photodynamic therapy in cells *in vitro* and tissues *in vivo*. Photochem Photobiol 2002;75:382–91.

46. Bensasson RV, Land EJ, Truscott TG. Excited states and free radicals in biology and medicine: contributions from flash photolysis and pulse radiolysis, New York: Oxford University Press Inc; 1993. p. 338–41.

47. Granville DJ, Carthy CM, Jiang H, Shore GC, McManus BM, Hunt DW. Rapid cytochrome *c* release, activation of caspases 3, 6, 7 and 8 followed by Bap31 cleavage in HeLa cells treated with photodynamic therapy. FEBS Lett 1998;437:5–10.

48. Granville DJ, Shaw JR, Leong S, et al. Release of cytochrome *c*, Bax migration, Bid cleavage, and activation of caspases 2, 3, 6, 7, 8, and 9 during endothelial cell apoptosis. Am J Pathol 1999;155:1021–5.

49. Runnels JM, Chen N, Ortel B, Kato D, Hasan T. BPD-MA-mediated photosensitization *in vitro* and *in vivo*: cellular adhesion and β1 integrin expression in ovarian cancer cells. Br J Cancer 1999;80:946–53.

50. Kessel D, Luo Y, Mathieu P, Reiners JJ Jr. Determinants of the apoptotic response to lysosomal photodamage. Photochem Photobiol 2000;71:196–200.

51. Berg K, Moan J. Lysosomes and microtubules as targets for photochemotherapy of cancer. Photochem Photobiol 1997;65:403–9.

52. Morgan J, Oseroff AR. Mitochondria-based photodynamic anticancer therapy. Adv Drug Deliv Rev 2001;49:71–86.

53. Moor AC. Signaling pathways in cell death and survival after photodynamic therapy. J Photochem Photobiol B 2000;57:1–13.

54. Tijerina M, Kopeckova P, Kopecek J. The effects of subcellular localization of *N*-(2-hydroxypropyl)methacrylamide copolymer-Mce(6) conjugates in a human ovarian carcinoma. J Control Release 2001;74: 269–73.

55. Putnam D, Kopecek J. Polymer conjugates with anticancer activity. Adv Polym Sci 1995;122:55–123.

56. Spiridon CI, Ghetie MA, Uhr J, et al. Targeting multiple Her-2 epitopes with monoclonal antibodies results in improved antigrowth activity of a human breast cancer cell line *in vitro* and *in vivo*. Clin Cancer Res 2002;8:1720–30.

57. Jung YD, Mansfield PF, Akagi M, et al. Effects of combination anti-vascular endothelial growth factor receptor and anti-epidermal growth factor receptor therapies on the growth of gastric cancer in a nude mouse model. Eur J Cancer 2002;38:1133–40.

58. Sands H. Experimental studies of radioimmunodetection of cancer: an overview. Cancer Res 1990;50:809–13s.

59. Jain RK. Physiological barriers to delivery of monoclonal antibodies and other macromolecules in tumors. Cancer Res 1990;50:814–9s.